

OPEN ACCESS

Hindered Aluminum Plating and Stripping in Urea/NMA/Al(OTF)₃ as a Cl-Free Electrolyte for Aluminum Batteries

To cite this article: Fatemehsadat Rahide *et al* 2023 *J. Electrochem. Soc.* **170** 120534

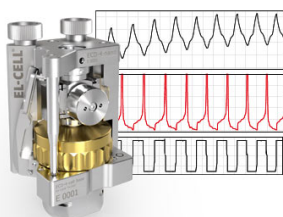
View the [article online](#) for updates and enhancements.

You may also like

- [Network meta-analysis: a statistical physics perspective](#)
Annabel L Davies and Tobias Galla
- [Open Challenges on Aluminum Triflate-Based Electrolytes for Aluminum Batteries](#)
Fatemehsadat Rahide, Eugen Zemlyanushin, Georg-Maximilian Bosch et al.
- [MILLIMETER RADIO CONTINUUM EMISSIONS AS THE ACTIVITY OF SUPERMASSIVE BLACK HOLES IN NEARBY EARLY-TYPE GALAXIES AND LOW-LUMINOSITY ACTIVE GALACTIC NUCLEI](#)
Akihiro Doi, Kouichiro Nakanishi, Hiroshi Nagai et al.

Measure the Electrode Expansion in the Nanometer Range. Discover the new ECD-4-nano!


electrochemical test equipment



- Battery Test Cell for Dilatometric Analysis (Expansion of Electrodes)
- Capacitive Displacement Sensor (Range 250 μm, Resolution ≤ 5 nm)
- Detect Thickness Changes of the Individual Electrode or the Full Cell.

www.el-cell.com +49 40 79012-734 sales@el-cell.com





Hindered Aluminum Plating and Stripping in Urea/NMA/Al(OTF)₃ as a Cl-Free Electrolyte for Aluminum Batteries

Fatemehsadat Rahide,^{1,z} Jackson K. Flowers,^{2,3} Junjie Hao,¹ Helge S. Stein,^{2,3} Helmut Ehrenberg,^{1,3} and Sonia Dsoke^{1,z}

¹Institute for Applied Materials (IAM), Karlsruhe Institute of Technology (KIT), 76344 Eggenstein-Leopoldshafen, Germany

²Institute of Physical Chemistry (IPC), Karlsruhe Institute of Technology (KIT), 76131 Karlsruhe, Germany

³Helmholtz Institute Ulm (HIU), 89081 Ulm, Germany

Conventional electrolytes for aluminum metal batteries are highly corrosive because they must remove the Al₂O₃ layer to enable plating and stripping. However, such corrosiveness impacts the stability of all cell parts, thus hampering the real application of aluminum-metal batteries. The urea/NMA/Al(OTF)₃ electrolyte is a non-corrosive alternative to the conventional [EMImCl]: AlCl₃ ionic liquid electrolyte (ILE). Unfortunately, this electrolyte demonstrates poor Al plating/stripping, probably because (being not corrosive) it cannot remove the Al₂O₃ passivation layer. This work proves that no plating/stripping occurs on the Al electrode despite modifying the Al surface. We highlight how urea/NMA/Al(OTF)₃ electrolyte and the state of the Al electrode surface impact the interphase layer formation and, consequently, the likelihood and reversibility of Al plating/stripping. We point up the requirement for carefully drying electrolyte mixture and components, as water results in hydrogen evolution reaction and creation of an insulating interphase layer containing Al(OH)₃, AlF₃, and re-passivated Al oxide, which finally blocks the path for the possible Al plating/stripping.

© 2023 The Author(s). Published on behalf of The Electrochemical Society by IOP Publishing Limited. This is an open access article distributed under the terms of the Creative Commons Attribution 4.0 License (<http://creativecommons.org/licenses/by/4.0/>), which permits unrestricted reuse of the work in any medium, provided the original work is properly cited. [DOI: 10.1149/1945-7111/ad1553]



Manuscript submitted May 26, 2023; revised manuscript received October 31, 2023. Published December 22, 2023.

Supplementary material for this article is available [online](#)

Aluminum batteries (AIBs) are considered a desirable alternative to lithium-ion batteries (LiBs) because Al, with a sustainable raw material supply owing to a mature Al foil industry¹ is recyclable, and abundant. Al metal has the highest theoretical volumetric specific capacity (8046 mAh cm⁻³)²⁻⁴ compared to other metals. Therefore, technologies based on Al anode can potentially bring high specific power and energy.³⁻⁵ AIBs can be classified into two main groups based on whether they utilize an aqueous or a non-aqueous electrolyte. The unsuccessful Al plating/stripping in aqueous electrolytes, due to the competitive H₂ evolution reaction, motivates scientists to search for alternative electrolytes that allow reversible Al plating/stripping. As a non-aqueous alternative, room-temperature ionic liquid electrolytes (RTILEs) with a wide electrochemical potential window and low vapor pressures are widely used in AIBs.^{6,7} The Al³⁺ cation does not exist in RTILEs, but Tetrachloroaluminate (AlCl₄⁻) and Heptachlorodialuminate (Al₂Cl₇⁻) anions exist, the latter being the only active species, which allow reversible Al plating/stripping.⁶ Several RTILEs have been reported,⁸⁻¹¹ but the most utilized non-aqueous ionic liquid electrolyte (ILE) compositions, which enable reversible Al plating/stripping, are melts based on imidazolium Chloride and AlCl₃.^{4,12} The commonly used Imidazole-based IL, a combination of 1-Ethyl-3-methylimidazolium chloride and Aluminum Chloride salts ([EMImCl]: AlCl₃ (1:1.5)), has good ionic conductivity and outstanding plating and stripping behavior.¹³ Its ability to successfully plate and strip Al is due to the presence of Al₂Cl₇⁻, which forms only when the molar ratio of AlCl₃ to [EMIm]Cl is higher than one.^{8,11,14} Although [EMImCl]: AlCl₃ is the most advanced chloroaluminate system for AIBs, attempts have been made to discover substitutes, as it is expensive, highly corrosive, hygroscopic, moisture-sensitive, and susceptible to hydrolysis.^{15,16} The most intuitive way to cope with chloroaluminate's reactivity is to use an alternative Cl-free electrolyte.¹⁶ Recently, many AlCl₃-free electrolytes (presented in Table I) have been explored, such as mixtures containing aluminum trifluoromethanesulfonate (Al(OTF)₃) and aluminum bis

(trifluoromethanesulfonyl)imide (Al(TFSI)₃) as non-corrosive alternative salts.

The urea/NMA/Al(OTF)₃ electrolyte shows an electrochemical stability window broader than [EMImCl]: AlCl₃,²⁶ but, unfortunately, it displays inadequate electrochemical Al plating/stripping on Al substrate, as demonstrated by our group.²⁷ Many other AlCl₃-free electrolytes (resumed in Table I) show poor performance in terms of plating and stripping. The Al(OTF)₃ salt shows poor plating and stripping not only in a mixture with urea and NMA, but also with other solvents like diglyme.^{20,21,26,27} Aluminum electrodeposition on molybdenum substrate from 1-butylimidazole bis(trifluoromethanesulfonyl) imide demonstrates quasi-reversible plating/stripping,¹⁷ but this is reversible only for a limited number of cycles or with significant side reactions. Al(TFSI)₃ in acetonitrile on molybdenum substrate and Al(PF₆)₃ in dimethyl sulfoxide on copper substrate show similar quasi-reversible behavior with significant plating/stripping overpotentials (> 1.5 V).^{17,18} To achieve successful Al plating/stripping in such non-corrosive environment, a proposed method is the modification of the aluminum anode (anode amorphization,²⁸ anode alloying,^{29,30} and surface modification³¹⁻³⁴) because the electrode-electrolyte interphase has a vital role for the plating/stripping process. The other method is the modification of the electrolyte by developing concentrated electrolytes,³⁵ adding water scavengers,^{36,37} and additives.^{25,38} Moreover, the amount of active Al species in the electrolyte influences the appearance of Al deposit.³ A chlorine-free electrolyte cannot ensure reversible Al plating/stripping without an appropriate and ionically conductive interphase, which can permit the Al plating/stripping process.^{15,39} This solid electrolyte interphase (SEI) can be created artificially (*ex situ*, prior cell assembly) or during the initial cell operation when the solvent's reduces and forms byproducts deposited on the anode surface.⁴⁰⁻⁴² The study of Loaiza, et al.³² revealed that the initial passivation layer formed upon contact with ILE is porous and intricate, comprised of an outer inorganic/organic layer and an inner oxide-rich layer. The cyclic stability of the cell can be improved by preventing additional solvent reduction and anode component disintegration by creating a stable and robust SEI layer (as it is well-known from the lithium battery technologies).^{9,34} Without this protection, byproducts of ILE

^zE-mail: fatemehsadat.rahide@kit.edu; sonia.dsoke@kit.edu

Table I. List of electrolyte compositions reported in the literature.

Electrolyte compositions	Working electrode	References
Al(OTF) ₃ /1-butyl-3-methylimidazolium trifluoromethanesulfonate ([BMIM]OTF)	Al	15
Al(TFSI) ₃ /acetonitrile	Mo	17
aluminum hexafluorophosphate (Al(PF ₆) ₃)/Dimethyl sulfoxide (DMSO)	Cu	18
aluminum trifluoromethanesulfonate (Al(OTF) ₃)/propylene carbonate/tetrahydrofuran (THF)		19
Al(OTF) ₃ /2-methoxy ethyl ether (diglyme)	Al	20, 21
Al(OTF) ₃ /THF	glassy carbon, and gold	22
Al(OTF) ₃ /LiCl/THF	gold	23
aluminum hexa-methylimidazole bis(trifluoromethansulfonyl)imide [Al(MIm) ₆]/[TFSI] ₃		
aluminum hexa-butylimidazole bis(trifluoromethansulfonyl)imide [Al(BIm) ₆]/[TFSI] ₃		
aluminum hexa-dimethyl sulfoxide [Al(DMSO) ₆]/[TFSI] ₃		
[Al(DMSO) ₆]/[OTF] ₃	Pt	24
Al(OTF) ₃ /tetrabutylammonium chloride (TBAC)/diglyme	Al	25
urea/Al(OTF) ₃ /N-methyl acetamide (NMA)	Pt	26

breakdown can be deposited again onto newly generated surfaces, and the interfaces may become unstable due to the ongoing process of dissolution and deposition.⁴³ However, regardless of the type of electrolyte, Al metal electrodes should serve as the state-of-the-art anode material in AIBs.^{4,13,32,44} It has been shown that the performance of AIBs is substantially influenced by the state of the Al foil surface and, in fact, electrode-electrolyte interphase.^{43–46} The ion-insulator Al₂O₃ oxide film covering the metallic Al anode blocks the anode's activation and makes it more difficult to attain a reversible reaction of Al plating and stripping, resulting in a substantial overpotential.^{3,32,43} However, at the same time, this passivation layer provides protection against ILE-induced corrosion, so a good balance between exposed and covered Al sites is desirable.^{32,47} Al₂O₃ oxide film can be dissolved locally, enabling adequate Al plating/stripping reaction when it is in contact with ILE^{44,47,48}; this can be considered as an Al surface modification that can be done before cell assembly. However, this modification as an extra and time-consuming step has hampered the development and real application of alternative and non-corrosive non-aqueous electrolytes.¹⁵ The Al₂O₃ passivation layer removal, as a surface modification, determines the reversibility of the Al plating/stripping at the electrode/electrolyte interface.^{14,15,47} Go et al.³⁴ claimed that the etched and electropolished Al foil has the greatest effect on AIBs' performance.³⁴ A surface pretreatment (as a type of surface modification) can typically be achieved by immersing the Al foil in ILE to partially remove or modify the Al₂O₃ passivation layer and build an Al, Cl, and N-rich layer at the surface,⁴⁷ thus creating an "artificial interphase".³⁹ Long et al.⁴⁹ demonstrated that, with this method, the dissolved Al₂O₃ oxide film in the ILE is replaced by an SEI layer rich in Cl and O species. On the other side, a complete removal of Al₂O₃ may be detrimental as this oxide prevents Al metal electrode disintegration.^{4,50} The morphological changes of Al metal as a function of immersion time in the ILE were also examined by Lee et al.,⁴³ who found that a new oxide layer with a particular lattice plane was grown on the Al surface. These findings confirmed that removing the thick oxide film layer during pretreatment is crucial for enhancing battery cell performance.¹⁵ However, the function of the native and electrolyte-derived passivation layer is still poorly understood despite its significant influence on the electrochemical performance of the Al anode, in both the aqueous⁵¹ and non-aqueous^{15,39,43,47} systems. In addition, the practical application of the active metallic Al anode material in urea/NMA/Al(OTF)₃ as a Cl-free non-corrosive electrolyte has not been evaluated, as no study on interphase layer formed on the Al anode has been reported. Therefore, our work aims to define the crucial issues hindering Al plating (on metallic aluminum) and the performance of surface (non-) modified Al anodes in a urea/NMA/Al(OTF)₃ electrolyte. With that, we highlight the bottlenecks of the urea/NMA/Al(OTF)₃ electrolyte in terms of Al plating/stripping on the Al substrate. The main issue may arise from hydrogen evolution reaction (HER) and the creation of interphase layer containing Al(OH)₃, Al-F, and re-passivated Al

oxide, which consequently blocks the path for Al ions through the electrode-electrolyte interphase.

Experimental

Materials.—In this study, anhydrous acetonitrile (99.8%) and anhydrous methanol (99.8%), anhydrous aluminum chloride (AlCl₃) (99.99%), and 1-Ethyl-3-methylimidazolium chloride (EMImCl) (95%) were purchased from Sigma Aldrich. A commonly used IL electrolyte in AIBs, [EMImCl]/AlCl₃ with a molar ratio of 1:1.5⁵² was prepared by gradually adding the calculated amount of AlCl₃ salt to the appropriate amount of EMImCl salt while stirring inside an argon-filled glovebox (MBraun, <0.5 ppm O₂, <0.5 ppm H₂O, temperature 28 to 30 °C). N-methylacetamide (NMA) (99%), urea (99%), aluminum trifluoromethanesulfonate (Al(OTF)₃) (99.9% trace metal basis), and molecular sieves (MS) of 3 Å (beads, 4 – 8 mesh) were all purchased from Sigma Aldrich. The initial measured water content in the as-received NMA solvent was about 4476 ppm; therefore, NMA was dried with MS for 10 days until the water content was less than 25 ppm as described in our previous paper.²⁷ A Karl Fisher titrator (Titroline® 7500 KF trace) was used to measure the water content. Urea and Al(OTF)₃ were vacuum-dried at 80 °C for 48 h in a glass oven (BÜCHI Glass Oven B-585) before being transferred to an argon-filled glovebox (MBraun, <0.5 ppm O₂, <0.5 ppm H₂O) and used later for the preparation of the urea/NMA/Al(OTF)₃ as reported in previous works.^{26,27} The molar ratio of urea/NMA/Al(OTF)₃ was 0.19:0.75:0.05. For the preparation of the urea/NMA/Al(OTF)₃ electrolyte, the required amounts of dried Al(OTF)₃ and urea were added to the melted (at 40 °C) NMA solvent while mixing and stirring with a magnet bar at room temperature inside the argon-filled glovebox.²⁷ The prepared [EMImCl]/AlCl₃ (**AlCl₃-based**) and urea/NMA/Al(OTF)₃ (**Al(OTF)₃-based**) electrolytes were kept sealed in the glovebox for the following electrochemical experiment. The aluminum (Al) foil (0.025 mm thickness and 99.0% purity) was purchased from Goodfellow. The platinum (Pt) foil (0.4 mm thickness and 99.9% purity) was provided by rhd Instruments GmbH & Co. KG (Germany).

Electrochemical setup.—All electrochemical cells were assembled/opened inside an argon-filled glovebox (MBraun, <0.5 ppm O₂, <0.5 ppm H₂O). The electrochemical techniques, including cyclic voltammetry (CV) and chronoamperometry (CA) have been applied in sealed, closed, and airtight TSC surface cells. The TSC surface cell was supplied by rhd Instruments GmbH & Co. KG (Germany). In this cell, an Al and a Pt foil were taken as working electrodes (WE, with a geometric area of 0.28 cm²), depending on the particular experiment. A glassy carbon (GC) disc was used as a counter electrode (CE, with 6 mm diameter), and an aluminum (Al) and silver (Ag) wire as quasi-reference electrodes. To avoid moisture in the cell, all cell auxiliaries were transported to the argon-filled glovebox after being dried in an

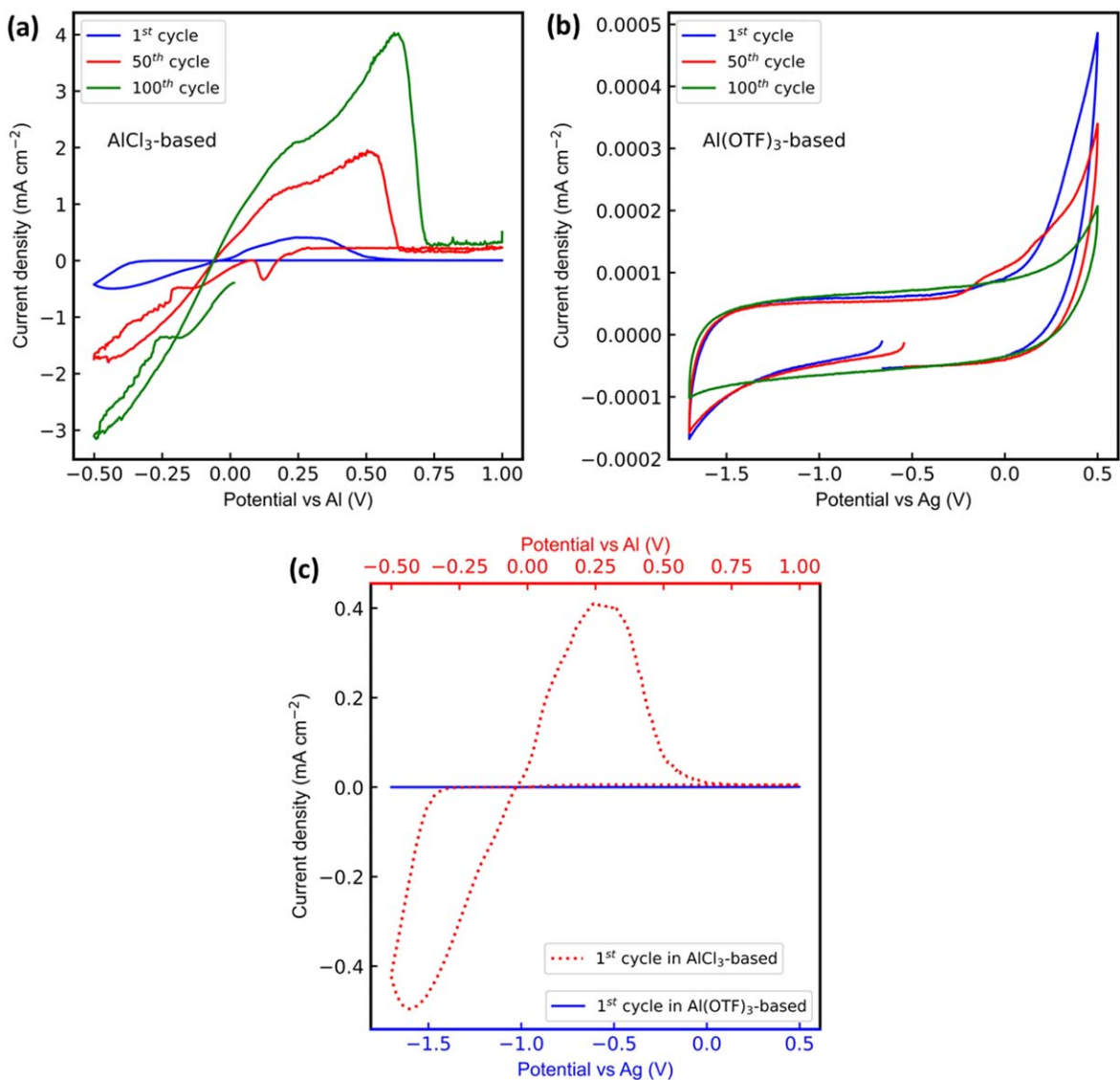


Figure 1. CVs recorded with a scan rate of 20 mV s^{-1} on pristine Al foil in (a) AlCl_3 -based electrolyte and (b) $\text{Al}(\text{OTF})_3$ -based (c) CVs comparison. Al and Ag wires are used as quasi-reference electrodes with AlCl_3 -based and $\text{Al}(\text{OTF})_3$ -based electrolytes, respectively.

oven at 80°C for 24 h before each cell assembly. Before and after each electrochemical test, the GC electrode was first polished with 250 nm diamond polishing paste, then rinsed in distilled water to remove any dirt or contamination from the electrode surface.²⁷ A mixture of $\text{H}_2\text{SO}_4/\text{H}_3\text{PO}_4/\text{HNO}_3$ (25/70/5 by volume) was used to polish and clean the Al quasi-reference electrode from any dirt and residual oxide.^{26,27} The Ag quasi-reference electrode was polished with a $1 \mu\text{m}$ diamond suspension and then rinsed in distilled water.²⁷ CVs and CAs were recorded with a biologic potentiostat (VMP12) at 25°C . CVs have been recorded with a scan rate of 20 mV s^{-1} in a potential range of -0.5 to 1.0 V vs. Al in AlCl_3 -based electrolyte, and in a potential range of -1.7 to 0.5 V vs. Ag in $\text{Al}(\text{OTF})_3$ -based electrolyte. Considering the stability window of the urea/NMA/ $\text{Al}(\text{OTF})_3$ electrolyte and the stability of the Ag quasi-reference electrode for Al plating and stripping, this potential range (-1.7 V to 0.5 V), was derived from prior study²⁷ where it had proven to be a reliable and effective window for Al electrodeposition and dissolution. It's notable to mention that according to the evidence, the calibration of the quasi-reference electrode showed notable shifts in the redox peaks of Ferrocene (utilized as an internal reference) against the Al wire. Conversely, using the Ag wire as the quasi-reference maintained a remarkably stable potential throughout the 24 h period.²⁷ CVs were carried out to study the possible Al reduction and oxidation reactions. CA with a constant

voltage of -1 V (vs. Ag in $\text{Al}(\text{OTF})_3$ -based electrolyte, and vs. Al in AlCl_3 -based electrolyte) for 5 h was performed to study the possible electroplated Al on the Al and Pt electrodes.

Ex-situ electrodes characterization.—All handling and preparation of the *ex situ* Al and Pt electrodes took place inside a glovebox filled with argon (MBraun, $<0.5 \text{ ppm O}_2$, $<0.5 \text{ ppm H}_2\text{O}$). To remove the residual electrolyte, surface-modified and cycled electrodes were rinsed in anhydrous acetonitrile or methanol, then dried for 12 h under a vacuum at room temperature in a glass oven (BÜCHI Glass Oven B-585). The pretreatment of the Al foil ($1 \text{ cm} \times 1 \text{ cm}$ with 0.025 mm thickness) was accomplished by immersion for 18 h in $900 \mu\text{l}$ of AlCl_3 -based electrolyte. The Pt foil after CA technique in AlCl_3 -based electrolyte, as well as the immersed Al electrode before being used as WE in $\text{Al}(\text{OTF})_3$ -based electrolyte, have been washed three times with anhydrous acetonitrile to make sure the residual electrolyte is removed and then vacuum-dried in a glass oven (BÜCHI Glass Oven B-585) at room temperature. The Al and Pt electrodes, after each applied electrochemical technique in $\text{Al}(\text{OTF})_3$ -based electrolyte, have been rinsed three times in fresh anhydrous methanol to remove the residual electrolyte and then dried under vacuum in a glass oven (BÜCHI Glass Oven B-585) at room temperature. Scanning electron microscope (SEM) imaging

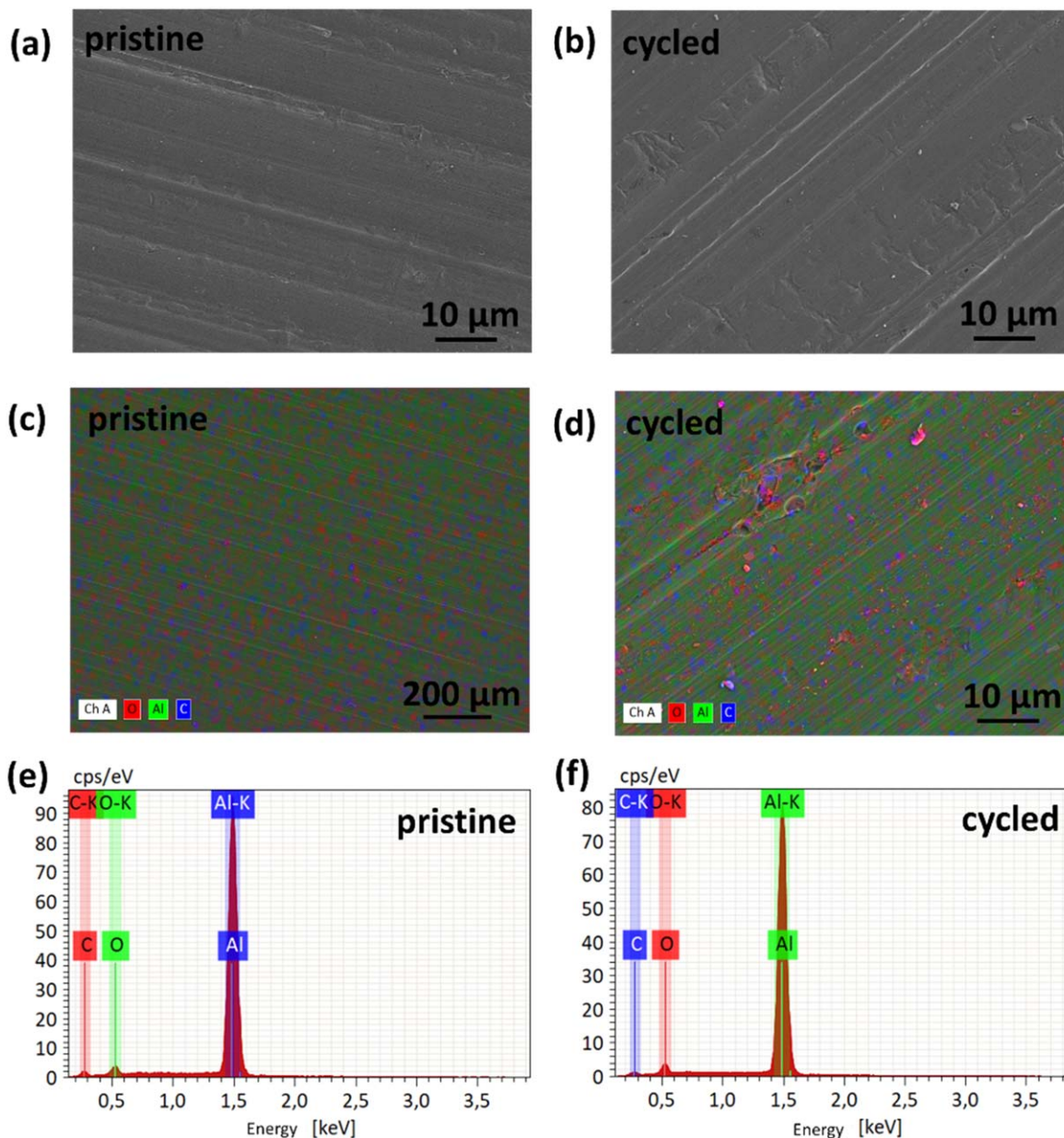


Figure 2. (a), (b) SEM images, (c)–(f) EDX images and spectra of the pristine and cycled Al foil in $\text{Al}(\text{OTF})_3$ -based electrolyte.

and energy-dispersive X-ray spectroscopy (EDX) of the Al and Pt electrodes were collected using a JEOL JSM 7500 F machine with acceleration voltages of 5 kV and 10 kV, respectively. The X-ray photoelectron spectroscopy (XPS) measurements of the Al and Pt electrodes were done with a Specs EnviroESCA NAP-XPS⁵³ (without making use of the near-ambient pressure (NAP) features, so at roughly 10^{-6} mbar) via a Nitrogen-filled glovebox (GS, <5 ppm O_2 , <0.5 ppm H_2O). More specifically, not using NAP features means that we are operating at the minimum of roughly 10^{-6} mbar, instead of the up to 10 mbar that the machine can reach. Survey spectra were taken with a pass energy of 100 eV and an energy resolution of 1 eV, while fine spectra were taken with a pass energy of 30 eV and a resolution of 0.1 eV.

Results and Discussion

Electrochemical characterization.—Figure 1 depicts the CVs recorded on the pristine Al foil in the $\text{Al}(\text{OTF})_3$ -based electrolyte. (Fig. 1b) shows that only capacitive current, i.e., no Al plating/

stripping reaction, can be observed on pristine Al foil in the $\text{Al}(\text{OTF})_3$ -based electrolyte. On the other hand, the Al redox reaction is visible on pristine Al foil in the AlCl_3 -based electrolyte (Fig. 1a). Concerning the AlCl_3 -based electrolyte, the peak current density related to Al stripping increases from 0.4 to 4.027 mAcm^{-2} from the 1st cycle to the 100th cycle, highlighting the activation process (which should imply progressive Al_2O_3 dissolution) as the cycle number increases. During the initial cycles, the native Al_2O_3 oxide film should have a few defect sites that allow electrolytes to pass through and react with internal Al below the cracks and defect sites.⁴ During the following cycles, the native Al_2O_3 oxide film gradually dissolves into the ILE since it cannot tolerate the acidic environment.³² At this point, the newly exposed portion of the Al foil begins to participate in the Al plating/stripping.⁴ The full progression of 100 CV cycles for both electrolytes is presented in Fig. S1. In agreement with the CV results, SEM images and EDX of the pristine and cycled Al electrode in $\text{Al}(\text{OTF})_3$ -based electrolyte reveal no change as no electrochemical reaction occurs on the Al electrode (Fig. 2). Complementary to SEM images, the observed elements of the pristine and cycled electrodes

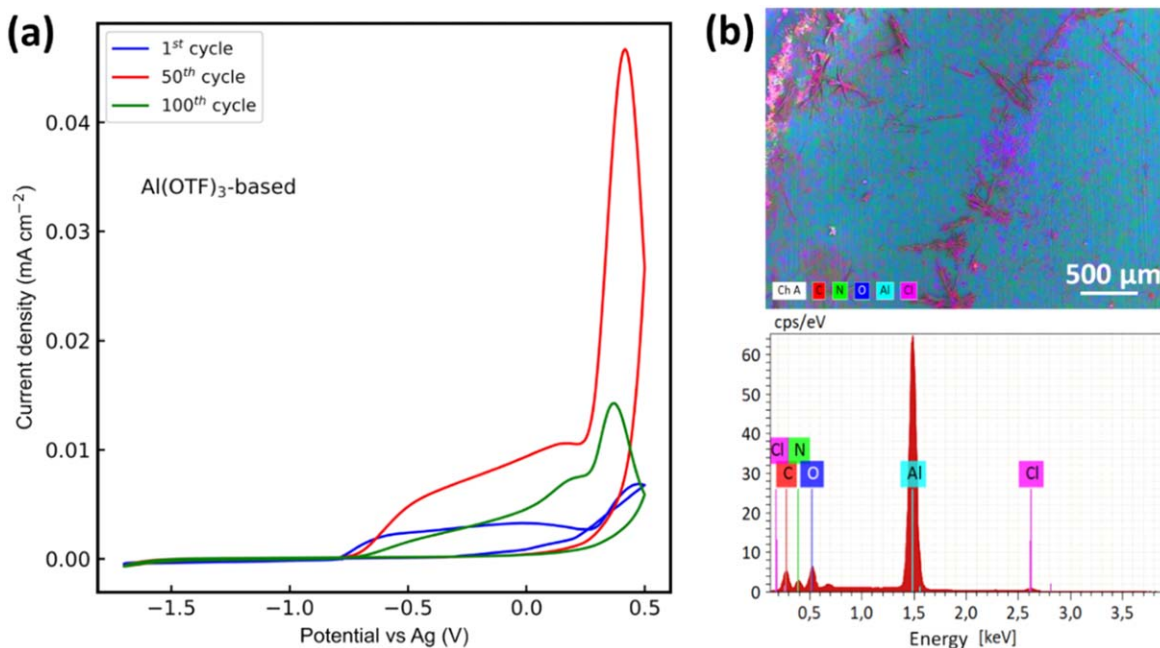


Figure 3. (a) CV recorded with a scan rate of 20 mV s^{-1} on MAI foil in $\text{Al}(\text{OTF})_3$ -based electrolyte. Ag wire is used as a quasi-reference electrode. (b) EDX results of cycled MAI foil.

are presented in Table S1. It is assumed that Al_2O_3 is not removed due to the non-acidic nature of the electrolyte therefore activation of Al plating/stripping has been impeded.^{1,17} Al_2O_3 oxide film dissolves in Lewis acidic $[\text{EMImCl}]/\text{AlCl}_3$ (1:1.5) electrolytes during cycling due to the existence of the chloroaluminate complexes, which explains the increase of the Al plating/stripping capacity with the cycle number. However, the Al_2O_3 oxide film deactivates the Al surface for any electrochemical reactions in the AlCl_3 -free electrolyte.¹⁵ This suggests that in the case of using $\text{Al}(\text{OTF})_3$ -based electrolyte, the Al surface must be modified by pretreatment¹⁵ to activate electrode-electrolyte interfaces for desired electrochemical reactions. Two crucial factors affect the possibility and reversibility of the Al plating/stripping process: 1) the appropriate electrode-electrolyte interphase driven by the state of Al_2O_3 oxide film covering the Al surface, 2) the water content of utilized electrolyte with the right ionic Al species. Therefore, firstly, we investigated if the state of the Al surface after 18 h of immersion in $900 \mu\text{l}$ of AlCl_3 -based electrolyte enables Al plating/stripping. Figure 3a shows the recorded CV on surface-modified Al (MAI) foil in $\text{Al}(\text{OTF})_3$ -based electrolyte. Figure 3b indicates the creation of an SEI rich in Al, N, Cl species during immersion pretreatment, and it agrees with previous studies.^{4,33,34} However, contrary to our expectation, no electrochemical activity can be observed for the MAI electrode. Although an oxidation peak with high current density is observed, no corresponding reduction peak is present, indicating that this is an irreversible reaction, as shown in Fig. 3b. This result is different from what was presented in $\text{Al}(\text{OTF})_3/[\text{BMIM}]\text{OTF}$ ionic liquid electrolyte by Wang et al.¹⁵ The reactivity of the Al surface and the $\text{Al}(\text{OTF})_3$ -based electrolyte with Cl^- ions form an insulating interphase layer resulting in a high anodic current density. In order to get more insight into the possible Al deposition in $\text{Al}(\text{OTF})_3$ -based electrolyte, we investigated the possibility of Al electrodeposition on a Pt working electrode²⁷ and then compared it with the electroplated Al on Pt from an AlCl_3 -based electrolyte. To achieve this goal, inspired by the work of Slim and Menke,²³ CA has been carried out to electroplate Al on Al and Pt electrodes from the electrolyte medium. Figure 4 shows CAs in the AlCl_3 -based and $\text{Al}(\text{OTF})_3$ -based electrolytes. Regardless of the electrolyte, a cathodic current appears during the CAs experiments. Oscillations in reductive currents during CAs could be attributed to the reductive decomposition of the anions in the AlCl_3 -based

electrolyte, as also observed by Slim et al. for other electrolyte compositions.²³ Furthermore, the XPS spectra of $\text{Cl}2p$ support this notion, indicating the continued bonding of chlorine to both aluminum and $[\text{EMIm}]^+$ (Fig. 5). Moreover, the recorded slow current reduction presented in Fig. 4a is probably due to the reduced active surface area of the Pt substrate and Al deposition.²³ The other reason could be the facilitation of further Al deposition from the electrolyte because of the freshly deposited Al^3 . XPS analysis of the Al and Pt electrodes was performed to see if the reductive current shown in Chronoamperograms correlates with the metallic Al deposition from active Al species of the electrolytes.

XPS analysis was performed on the three electrodes: a Pt foil, which had undergone CA to electroplate Al from an AlCl_3 -based electrolyte, and on Al and Pt electrodes after CA in an $\text{Al}(\text{OTF})_3$ -based electrolyte. All spectra were analyzed in CasaXPS. Fits of the spectrum for each element and each electrode are shown in Figs. 5–7. The lists of peaks for each spectrum are shown in Tables S2–S4. The surface of the Pt foil after Al electroplating with AlCl_3 -based electrolyte was thickly covered with Al deposition products. Thus, as expected, Pt is not visible in the XPS spectrum. Fine spectra were performed on the $\text{Cl}1s$, $\text{N}1s$, $\text{O}1s$, $\text{Al}2p$, and $\text{Cl}2p$ regions and presented in Fig. 5. The Al peaks are clearly bimodal, with the two $\text{Al}2p_{3/2}$ peaks occurring at 74.6 and 71.6 eV, due to Al^{3+} and Al metal respectively. The $\text{Cl}2p$ spectrum contains two overlapping doublets, demonstrating that chlorine remains bonded to both aluminum and $[\text{EMIm}]$. The AlCl_3 $\text{Cl}2p_{3/2}$ occurs at 198.7 eV and that of $[\text{EMIm}]\text{Cl}$ at 197.6 eV, consistent with the results of Calisi et al.⁵⁴ The $\text{Cl}1s$ spectrum was fit with three peaks: a C–C/C–H peak, which was calibrated to 285 eV, a C–O/C–N peak at 286.1 eV, and an O–C=O peak at 289.1 eV. The $\text{N}1s$ spectrum displays a larger peak at 401.7 eV coming from cationic nitrogen in imidazolium,⁵⁵ and a smaller neutral C–N peak at 399.9 eV, showing either a decomposition product of the imidazolium or residual acetonitrile from washing. Finally, the $\text{O}1s$ spectrum is fit with two overlapping peaks, a smaller peak at 530.8 eV, and a much larger one at 532.2 eV. In summary, we reconfirm $[\text{EMImCl}]/\text{AlCl}_3$ as an effective electrolyte for Al plating,⁵⁶ and the $\text{O}1s$ peak at 532.2 eV suggests that the primary surface Al^{3+} compound in the sample is $\text{Al}(\text{OH})_3$.⁵⁷ This significant hydroxide

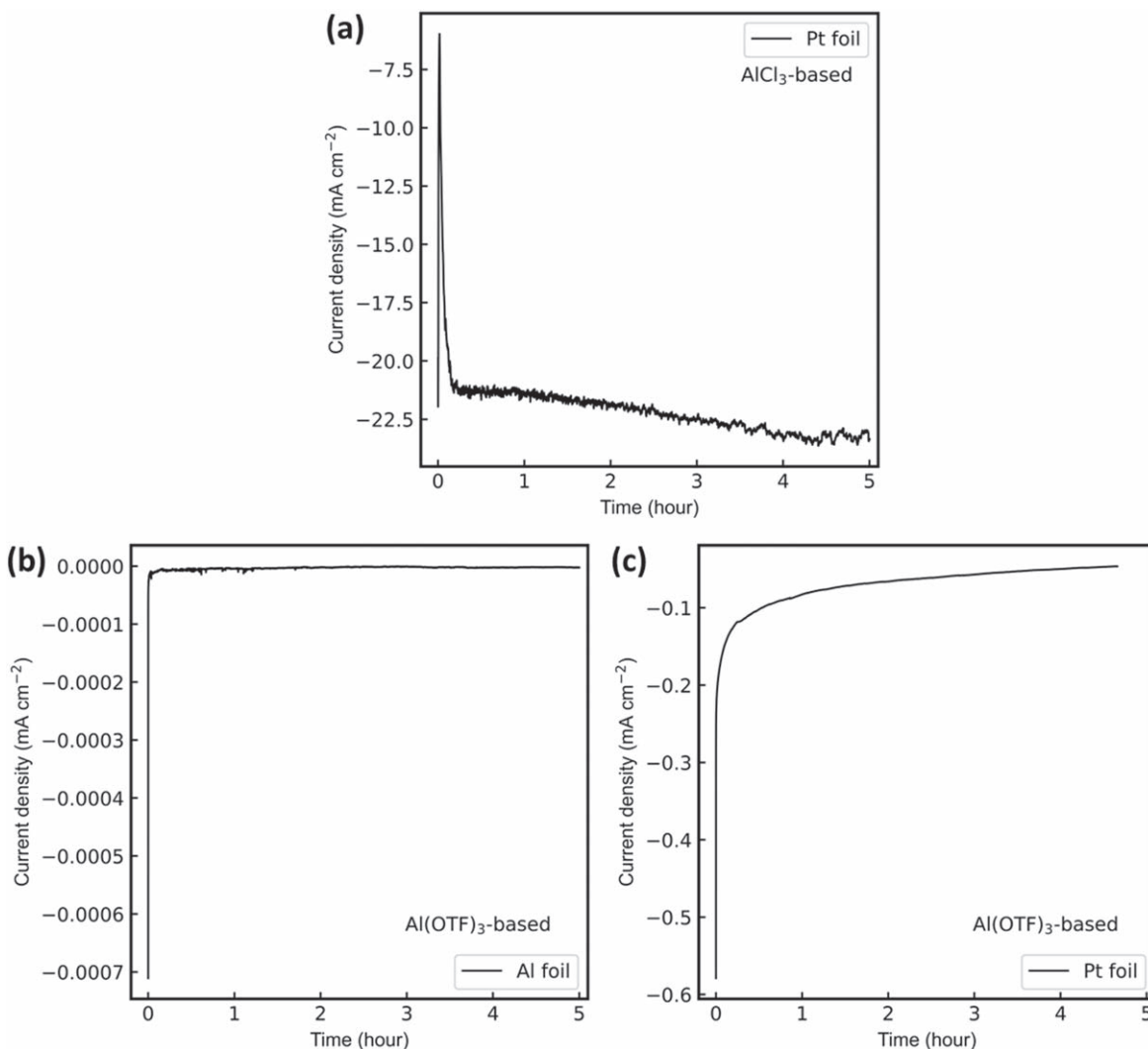


Figure 4. Chronoamperograms recorded at -1 V, corresponding to Al deposition on Pt electrode from (a) AlCl_3 -based electrolyte and on (b) Pt (c) Al electrode from $\text{Al}(\text{OTF})_3$ -based electrolyte. Al and Ag wires are used as quasi-reference electrodes.

peak observed on the surface might stem from the glovebox atmosphere. The intricate composition of the oxide passivation layer on the Al metal surface is susceptible to alterations caused by storage conditions.^{58,59} Factors such as temperature and humidity impact the absorption of elements like water, hydroxides, and carbon dioxide, thereby influencing the layer's overall composition.⁵⁸ It's notable that the observed fluctuation in CV (Fig. 1a) can be attributed to the uneven current distribution across the electrode surface, highlighting the possibility of gas evolution from the Al metal's surface during cycling. This connection aligns with XPS observations, reinforcing the correlation between current distribution and gas evolution due to the presence of $\text{Al}(\text{OH})_3$. Moreover, this fluctuation is directly proportional to the scan rate.

Analysis of the Al electrode after CA measurement in $\text{Al}(\text{OTF})_3$ -based electrolyte was complicated by the impossibility of distinguishing deposited Al metal from that already present on the sample. Visually, the measured Al foil lacks the thick deposition layer visible on the Pt foil. Fine spectra were taken for $\text{F}1s$, $\text{O}1s$, $\text{C}1s$, and $\text{Al}2p$. The $\text{Al}2p$ spectrum shows again two doublets, ascribed to Al metal and Al^{3+} . The $\text{O}1s$ splits into two peaks, at 532.3 eV and at 531.1 eV, which are again attributed to $\text{Al}(\text{OH})_3/\text{C}-\text{O}$ and $\text{Al}_2\text{O}_3/\text{O}-\text{C}=\text{O}$.⁵⁷ The $\text{C}1s$ spectrum contains a number of well-defined peaks at 285, 285.8, 289.5, 293.1, and 296.3 eV. The first four of these are assigned to $\text{C}-\text{C}$, $\text{C}-\text{O}$, $\text{O}-\text{C}=\text{O}$

$\text{C}-\text{F}$, and $-\text{CF}_3$, respectively, with the $\text{C}-\text{F}$ compounds clearly derived from the reduction of OTF. The peak at 296.3 eV is tentatively assigned to CF_4 ,⁶⁰ but may just be a satellite structure. The $\text{F}1s$ spectrum has two peaks: a larger one at 688.7 eV, which is also characteristic of $\text{C}-\text{F}$ bonding, and a smaller one at 685.6 eV, which is ascribed to a minuscule amount of AlF_3 ,⁶¹ though any corresponding peak in the $\text{Al}2p$ spectrum is too small to be resolved. The observed AlF_3 results from the reduction of OTF^- anion containing fluorine.^{39,62,63} Moreover, AlF_3 participates in the "re-passivation" process and may cause overpotential of the HER over time.³⁹ We verified that, although the components have been dried as reported in previous,²⁷ high water content (about 28466 ppm) was still present in the $\text{Al}(\text{OTF})_3$ -based electrolyte. Another H_2 source could also arise from the decomposition of urea.²⁷ Thermodynamically and kinetically, an excess of $\text{H}^+/\text{H}_3\text{O}^+$ assists even in the earlier onset of hydrogen evolution,⁶⁴ which may explain the trace hydroxide present in the sample. We assume that the water content is produced during electrolyte preparation, as all electrolyte components have been vacuumed and dried before the electrolyte preparation, as previously reported in the literature.²⁷ However, the presence of water and its effect on $\text{Al}(\text{OTF})_3$ -based electrolytes have not been explored before^{24,26}. This high water content would interfere with Al plating⁴¹ because water in the electrolyte solution would result in HER in the presence of Al: As a primary cathodic

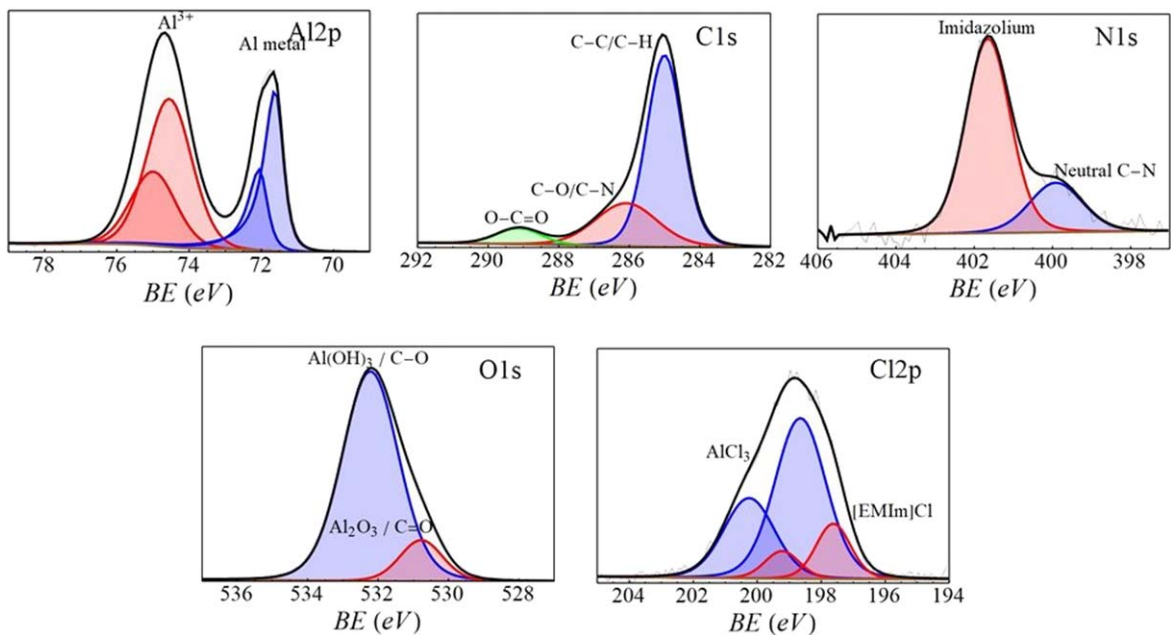


Figure 5. XPS fine spectra with peak assignments for Pt foil after Al electrodeposition from AlCl_3 -based electrolyte. Intensities are normalized for each spectrum individually.

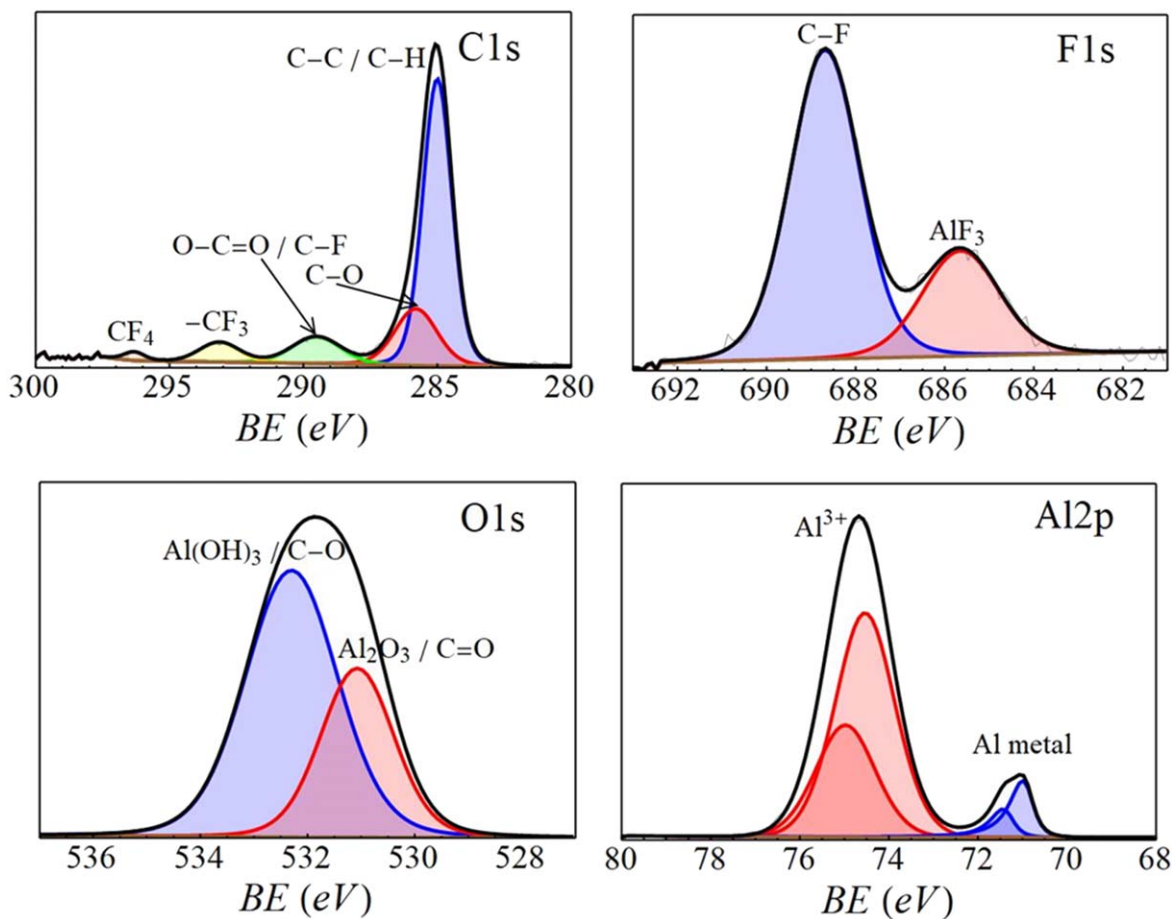


Figure 6. XPS fine spectra with peak assignments for Al electrode after applied chronoamperometry technique in $\text{Al}(\text{OTF})_3$ -based electrolyte. Intensities are normalized for each spectrum individually.

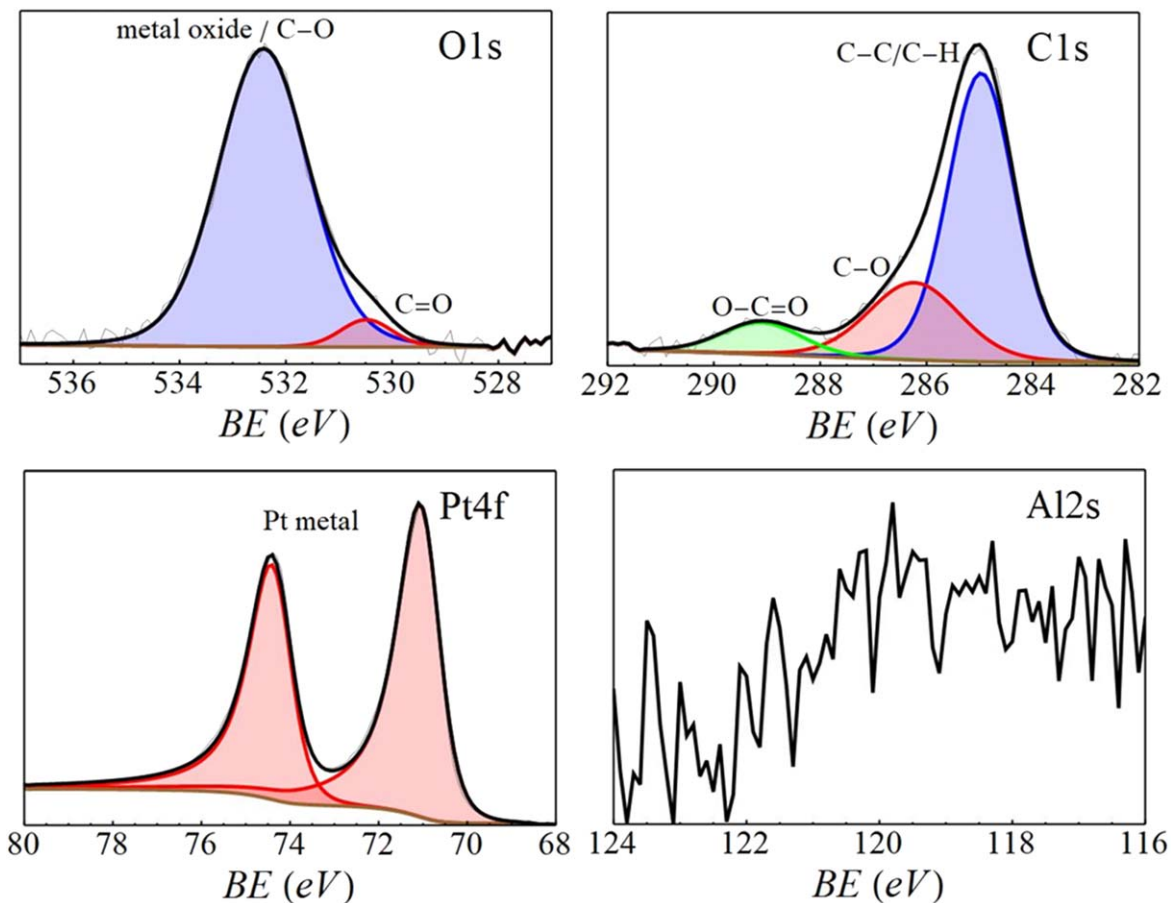


Figure 7. XPS fine spectra with peak assignments for Pt electrode after applied chronoamperometry technique in $\text{Al}(\text{OTF})_3$ -based electrolyte. Intensities are normalized for each spectrum individually. Note that energy window of the Pt4f spectrum does not extend far enough to capture the full asymmetric tail.

reaction, the HER ($2\text{Al} + 6\text{H}_2\text{O} \rightarrow 2\text{Al}(\text{OH})_3 + 3\text{H}_2$) prevents the possibility of reversible Al plating and stripping.⁴¹ Water molecules serve as a source of oxygen for the creation of oxide films.⁶⁵

The oxide film is also re-passivated when the organic component degrades or dissolves in the electrolyte, although the first oxide layer should be much less uniform and probably thinner than those on pristine aluminum. Passive oxide film production also occurs in the pH-neutral range (4 to 8).¹⁶ As shown in Fig. S2, the measured pH of the electrolyte is attributed to the polarized O-H bonds of water molecules coordinating Al^{3+} .^{39,66} The Al^{3+} transport would be hindered by the formed SEI containing AlF_3 , $\text{Al}(\text{OH})_3$, and re-passivated Al oxide. We should also note that the Al-metal peak is not notably enhanced compared to untreated samples, and the O1s structure shows a mixture of oxide and hydroxide similar to what we have seen in pristine foil samples. It is thus also possible that the oxide-hydroxide layer of the pristine foil was not attacked at all, or that the oxide layer could have formed from trace oxygen and water between cycling and measurement. Regardless of the cause, given the highly regular character of the oxide layer, and low concentration of electrolyte deposition products, we infer that significant Al-deposition did not take place. A summary and approximate breakdown of the relative signal between spectra can be found in Table S3.

Finally, Pt foil, which had undergone CA to electroplate Al from $\text{Al}(\text{OTF})_3$ -based electrolyte, shows nothing indicating any interaction with the electrolyte. Only Pt metal is observed, with trace impurities and adventitious carbon on the surface. This result apparently contradicts the reduction current seen in a recorded CV at a Pt electrode.²⁷ However, this current could derive from

hydrogen evolution via the electrochemical reduction of urea since the overpotential for hydrogen evolution is low at Pt electrode substrates and it is currently under investigation in our group. A summary and approximate breakdown of the relative signal between spectra can be found in Table S4.


Conclusion and outlooks.—The recorded CVs on pristine and surface-modified Al foil reveal a lack of any successful Al plating/stripping in $\text{Al}(\text{OTF})_3$ -based electrolyte. XPS analysis of the electrodeposited Al on Pt electrode from AlCl_3 -based electrolyte indicates significant deposition of Al metal. Al metal may undergo oxidation after deposition. Concerning the $\text{Al}(\text{OTF})_3$ -based electrolyte, XPS analysis of the Al and Pt electrodes reveals no electroplated Al. The evident trace of the electrolyte is a small proportion of C-F compounds, related to the reduction of OTF. In addition, the created interphase layer on Al electrode containing AlF_3 , $\text{Al}(\text{OH})_3$, and re-passivated Al oxide correlates with occurred HER owing to the high amount of water content in the electrolyte, despite the electrolyte components have been dried as reported in the literature.²⁷ It is confirmed that the hindered Al plating is due to the formed insulating interphase layer containing AlF_3 , $\text{Al}(\text{OH})_3$, and re-passivated Al oxide. XPS analysis of the Pt electrode after CA in $\text{Al}(\text{OTF})_3$ -based electrolyte shows no measurable deposition of any electrolyte material. As an outlook of the presented study, the contribution of the electrolyte should be explored more in terms of the other possible side reactions aside from the HER and $\text{Al}(\text{OTF})_3$ degradation. A better approach to reduce the interaction between Al and H_2O is the addition of water scavengers or additives, water-binding polymers, and additive-driven interfacial engineering.

Acknowledgments

The authors thank Dr Sebastian Kranz, Dr Benedikt Huber, and Dr Marcel Drüschler of the rhd instruments company for their scientific support and assistance in battery cell setup supplies. This work contributes to the research performed at CELEST (Center for Electrochemical Energy Storage Ulm-Karlsruhe) and was funded by the German Research Foundation (DFG) under Project ID 390874152 (POLiS Cluster of Excellence). Data availability. The data that support the findings of this study are openly available in KIT Library at <http://doi.org/10.35097/1785>. Conflict of interest. The authors declare no conflict of interest.

ORCID

Fatemehsadat Rahide  <https://orcid.org/0009-0003-8157-7927>

Sonia Dsoke  <https://orcid.org/0000-0001-9295-2110>

References

- S. K. Das, S. Mahapatra, and H. Lahan, *J Mater Chem A Mater*, **5**, 6347 (2017).
- Y. Zhang, S. Liu, Y. Ji, J. Ma, and H. Yu, *Adv. Mater.*, **30**, 1706310 (2018).
- Q. Li and N. J. Bjerrum, *J. Power Sources*, **110**, 1 (2002).
- E.-S. Lee, S.-H. Huh, S.-H. Lee, and S.-H. Yu, *ACS Sustain Chem Eng*, **11**, 2014 (2023).
- B. Craig, T. Schoetz, A. Cruden, and C. Ponce de Leon, *Renew. Sustain. Energy Rev.*, **133**, 110100 (2020).
- Z. J. Karpinski and R. A. Osteryoung, *Inorg. Chem.*, **23**, 1491 (1984).
- N. Takami and N. Koura, *Electrochim. Acta*, **33**, 1137 (1988).
- P. R. Gifford and J. B. Palmisano, *J. Electrochem. Soc.*, **135**, 650 (1988).
- S. Das, S. S. Manna, and B. Pathak, *ACS Appl. Energy Mater.*, **5**, 13398 (2022).
- S. Das, S. S. Manna, and B. Pathak, *ACS Omega*, **6**, 1043 (2021).
- M. Walter, M. V. Kovalenko, and K. V. Kravchuk, *New J. Chem.*, **44**, 1677 (2020).
- M.-C. Lin et al., *Nature*, **520**, 324 (2015).
- D. Muñoz-Torrero, J. Palma, R. Marcilla, and E. Ventosa, *Dalton Trans.*, **48**, 9906 (2019).
- T. Jiang, M. J. Chollier Brym, G. Dubé, A. Lasia, and G. M. Brisard, *Surf. Coat. Technol.*, **201**, 1 (2006).
- H. Wang et al., *ACS Appl. Mater. Interfaces*, **8**, 27444 (2016).
- G. A. Elia et al., *Adv. Mater.*, **28**, 7564 (2016).
- M. Chiku, S. Matsumura, H. Takeda, E. Higuchi, and H. Inoue, *J. Electrochem. Soc.*, **164**, A1841 (2017).
- X. Wen et al., *J. Phys. Chem. Lett.*, **12**, 5903 (2021).
- N. Jayaprakash, S. K. Das, and L. A. Archer, *Chem. Commun.*, **47**, 12610 (2011).
- L. D. Reed, S. N. Ortiz, M. Xiong, and E. J. Menke, *Chem. Commun.*, **51**, 14397 (2015).
- L. D. Reed, A. Arteaga, and E. J. Menke, *J. Phys. Chem. B*, **119**, 12677 (2015).
- Z. Slim and E. J. Menke, *J. Phys. Chem. B*, **124**, 5002 (2020).
- Z. Slim and E. J. Menke, *J. Phys. Chem. C*, **126**, 2365 (2022).
- T. Mandai and P. Johansson, *J. Phys. Chem. C*, **120**, 21285 (2016).
- S. Kumar et al., *Nanomicro Lett.*, **15**, 21 (2023).
- T. Mandai and P. Johansson, *J Mater Chem A Mater*, **3**, 12230 (2015).
- F. Rahide, E. Zemlyanushin, G.-M. Bosch, and S. Dsoke, *J. Electrochem. Soc.*, **170**, 030546 (2023).
- C. Yan et al., *J. Am. Chem. Soc.*, **144**, 11444 (2022).
- Q. Ran et al., *Nat. Commun.*, **13**, 576 (2022).
- G. Razaz et al., *Materials*, **16**, 933 (2023).
- D. Pradhan, D. Mantha, and R. G. Reddy, *Electrochim. Acta*, **54**, 6661 (2009).
- L. C. Loaiza, N. Lindahl, and P. Johansson, *J. Electrochem. Soc.*, **170**, 030512 (2023).
- D.-M. She et al., *J. Electrochem. Soc.*, **167**, 130530 (2020).
- H. Go, M. R. Raj, Y. Tak, and G. Lee, *Electroanalysis*, **34**, 1308 (2022).
- A. Zhou et al., *ACS Appl. Mater. Interfaces*, **11**, 41356 (2019).
- R. Horia, D.-T. Nguyen, A. Y. S. Eng, and Z. W. Seh, *Nano Lett.*, **21**, 8220 (2021).
- I. Weber, J. Ingenmey, J. Schnaidt, B. Kirchner, and R. J. Behm, *ChemElectroChem*, **8**, 390 (2021).
- D.-T. Nguyen et al., *Energy Storage Mater.*, **45**, 1120 (2022).
- Q. Zhao et al., *Sci. Adv.*, **4**, eaau8131 (2018).
- E. Peled, *J. Electrochem. Soc.*, **126**, 2047 (1979).
- T. Dong, K. L. Ng, Y. Wang, O. Voznyy, and G. Azimi, *Adv. Energy Mater.*, **11**, 2100077 (2021).
- A. Wang, S. Kadam, H. Li, S. Shi, and Y. Qi, *NPJ Comput. Mater.*, **4**, 15 (2018).
- D. Lee, G. Lee, and Y. Tak, *Nanotechnology*, **29**, 36LT01 (2018).
- S. Choi, H. Go, G. Lee, and Y. Tak, *Phys. Chem. Chem. Phys.*, **19**, 8653 (2017).
- A. Eftekhari and P. Corrochano, *Sustain Energy Fuels*, **1**, 1246 (2017).
- M. Jiang et al., *Adv. Mater.*, **34**, 2102026 (2022).
- F. Rahide et al., *ChemSusChem*, e202301142 (2023).
- D. Muñoz-Torrero et al., *J. Power Sources*, **374**, 77 (2018).
- Y. Long et al., *Energy Storage Mater.*, **34**, 194 (2021).
- H. Chen et al., *ACS Appl. Mater. Interfaces*, **9**, 22628 (2017).
- S. Kumar, V. Verma, H. Arora, W. Manalastas, and M. Srinivasan, *ACS Appl. Energy Mater.*, **3**, 8627 (2020).
- G. A. Elia et al., *J Mater Chem A Mater*, **5**, 9682 (2017).
- P. M. Dietrich, S. Bahr, T. Yamamoto, M. Meyer, and A. Thissen, *J Electron Spectros Relat Phenomena*, **231**, 118 (2019).
- N. Calisi et al., *J Electron Spectros Relat Phenomena*, **247**, 147034 (2021).
- S. Caporali, U. Bardi, and A. Lavacchi, *J Electron Spectros Relat Phenomena*, **151**, 4 (2006).
- J. Tu et al., *Chem. Rev.*, **121**, 4903 (2021).
- J. van den Brand, W. G. Sloof, H. Terryn, and J. H. W. de Wit, *Surf. Interface Anal.*, **36**, 81 (2004).
- M. Textor and M. Amstutz, *Anal. Chim. Acta*, **297**, 15 (1994).
- L. C. Loaiza, N. Lindahl, and P. Johansson, *J. Electrochem. Soc.*, **170**, 030512 (2023).
- A. V. Naumkin and A. Kraut-Vass, *NIST X-ray Photoelectron Spectroscopy Database, National Institute of Standards and Technology* (National Institute of Standards and Technology, Gaithersburg MD) (2008).
- D. Briggs, *Surf. Interface Anal.*, **3** (1981).
- L. Suo et al., *Science (1979)*, **350**, 938 (2015).
- L. Suo et al., *Adv. Energy Mater.*, **7**, 1701189 (2017).
- Z. Liu et al., *Chem. Soc. Rev.*, **49**, 180 (2020).
- D. D. Macdonald, *Electrochim. Acta*, **56**, 1761 (2011).
- F. Wang et al., *Nat. Mater.*, **17**, 543 (2018).